Bio-Inspired Multistructured Conical Copper Wires for Highly Efficient Liquid Manipulation

Qianbin Wang,[†] Qingan Meng,[†] Ming Chen,[†] Huan Liu,[†,*] and Lei Jiang[†,‡]

[†]Key Laboratory of Bio-Inspired Smart Interfacial Science and Technology of Ministry of Education, School of Chemistry and Environment, Beihang University, Beijing 100191, P. R. China and [‡]Beijing National Laboratory for Molecular Sciences (BNLMS), Key Laboratory of Organic Solids, Institute of Chemistry, Chinese Academy of Sciences, Beijing 100190, P. R. China

ABSTRACT Animal hairs are typical structured conical fibers ubiquitous in natural system that enable the manipulation of low viscosity liquid in a well-controlled manner, which serves as the fundamental structure in Chinese brush for ink delivery in a controllable manner. Here, drawing inspiration from these structure, we developed a dynamic electrochemical method that enables fabricating the anisotropic multiscale structured conical copper wire (SCCW) with controllable conicity and surface morphology. The as-prepared SCCW exhibits a unique ability for manipulating liquid with significantly high efficiency, and over 428 times greater than its own volume of liquid could be therefore operated. We propose that the boundary condition of the dynamic liquid balance behavior on conical fibers, namely, steady holding of liquid droplet at the tip region of the SCCW, makes it an excellent fibrous medium to manipulate liquid. Moreover, we demonstrate that the titling angle of the SCCW can also affect its efficiency of liquid manipulation by virtue of its mechanical rigidity, which is hardly realized by flexible natural hairs. We envision that the bio-inspired SCCW could give inspiration in designing materials and devices to manipulate liquid in a more controllable way and with high efficiency.

KEYWORDS: bio-inspired · liquid manipulation · conical shape · multistructured scale · highly efficient

The manipulation of liquid droplets, especially those in a controlled manner, is significantly important in various fields such as printing or patterning,[1−4] bio-assays,[5−7] nanomaterial fabrication,[8−10] aerosol-removal of filters,[11−13] and chemical reactions.[14−16] Generally, fluid is principally handled by using components such as channels,[17] nozzles,[18] or tubes,[19] where the fluidic mobility is restricted or guided in certain way by using a solid to enclose the transported liquid physically. Despite the popularity of these closed systems, their typical confined geometry pose several challenges, such as high flow resistance and propensity to clogging. Open systems, especially the fibrous media,[11,20,21] appear to be attractive alternatives in manipulating liquid because of their lower hydrodynamic resistance and ease in fabrication and processing.[13,22] For example, it has been reported that the flexible fiber array enables manipulation of silicon oil drop in various ways depending on elastocapillary imbibition,[11] the rigid nanowires can continuously pump liquid moving on their outer surfaces, and [23] the spider silks and the cacti are capable of collecting tiny water droplets efficiently from humid air.[24,25] Drawing inspirations from these examples in nature, numerous artificial fibrous systems with special liquid manipulation abilities were developed from both organic and inorganic materials. We recently fabricated artificial spider silks from polymer of PMMA, PVAc, PS, PVDF, *etc.*[20,26] and conical copper wires with gradient wettability[27] to realize water harvesting from humid air. It was also reported that the polymer conical needle arrays enable separation of micro-sized oil droplets from water.[12] So far, most researchers have focused on the self-propelling behavior of liquid droplets on conical fibers that was driven by the surface physicochemical gradient, whereas the efficiency of liquid transfer was seldom mentioned. In addition, it has been well documented that the conical structure, *i.e.*, structural asymmetry, is the key to drive the self-propelling of water droplet on the conical fibers, but

* Address correspondence to liuh@buaa.edu.cn.

Received for review June 25, 2014 and accepted July 22, 2014.

Published online July 22, 2014
10.1021/nn503463y

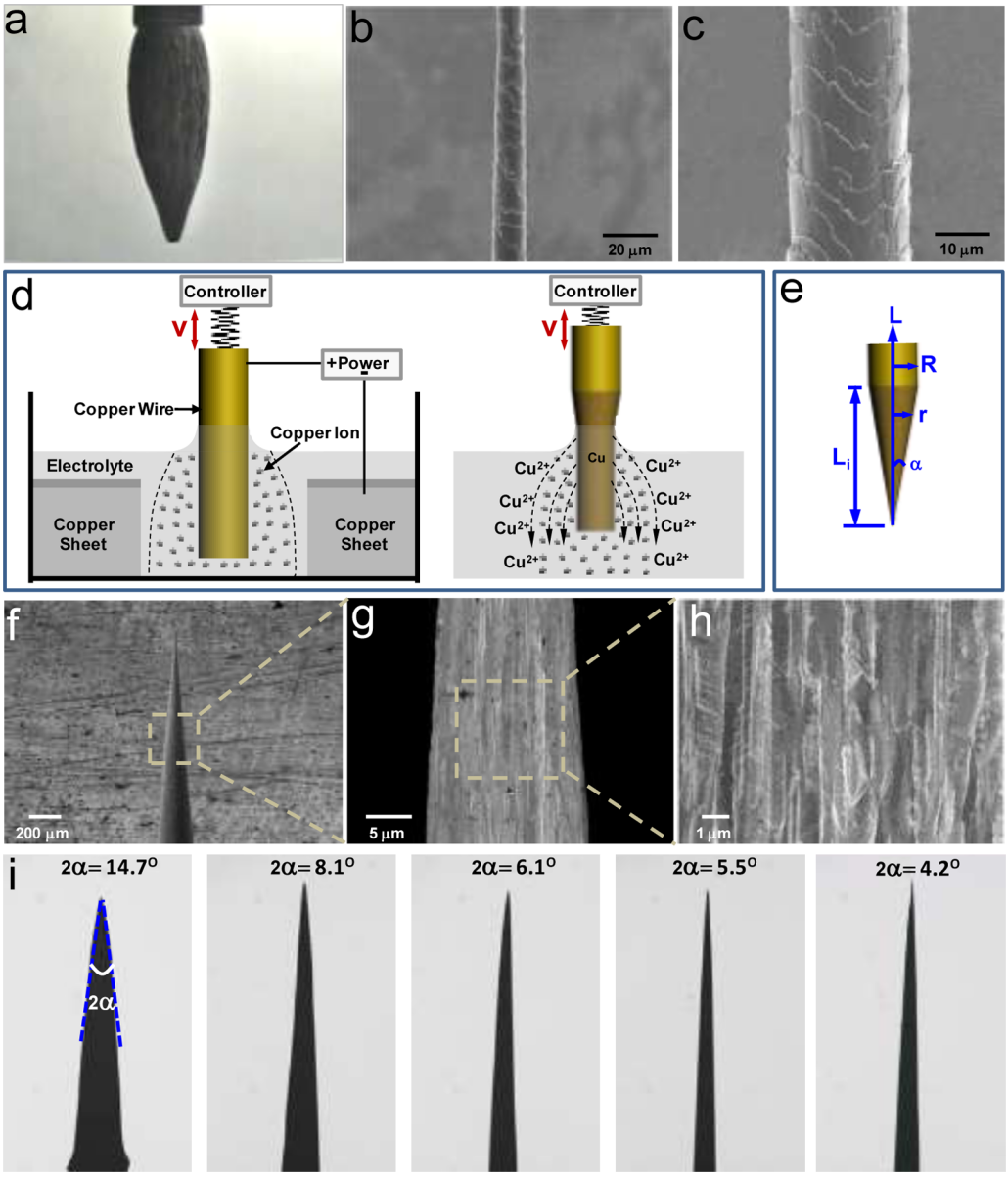

Figure 1. Chinese brush inspired structured conical copper wires. (a–c) A Chinese brush has the ability to store a large mass of ink in a well-controlled manner (a), which is contributed to the freshly emergent hairs with tapered architecture (b) enveloped by oriented micrometer scaled squamae (c). (d and e) A dynamic electrochemical method was used to controllably fabricate the bio-inspired, surface-structured conical copper wire (SCCW). (f–h) Scanning electron microscopy (SEM) images of a SCCW indicated its hierarchical micro-/nanostructures, featured by the conical architecture with micrometer scaled grooves and nanostructured scales. (i) When we adjust the length of the immersed wire, SCCWs with various apex angles of 2α can be precisely fabricated in a well-controllable way.

how the structural asymmetry can affect the ability of conical fibers in handling liquid droplet has been minimally reported so far, mainly because of the difficulty in fabricating conical fibers with controllable topography and morphology. Manipulating liquid in a well-controlled way and with high efficiency by a fibrous system is rarely reported, and the mechanism is poorly understood.

As a typical structured conical fiber that widely existed in natural system, freshly emergent hair (FE-hair), either in bundles or arrays, enables manipulation of a large amount of low viscosity liquid in a well-controlled manner (Figure 1a). We recently reported that the outstanding ability in manipulating liquid of FE-hair is assignable to its unique anisotropic multiscale structures, featured by the tapered architecture with conical tip covered with oriented micrometer scaled squamae (Figure 1b,c).[28] The cooperative effect of the Laplace pressure difference (ΔP) generated by the conical structure,[12,24,25,29] the asymmetrical retention force aroused from oriented squamae[30–33] and gravity, makes it possible for a Chinese brush to hold a large quantity of low viscosity ink liquid and to transfer the liquid onto the substrate in a controlled manner.

Herein, inspired by the animals' FE-hairs, we developed a dynamic electrochemical approach to fabricate a surface-structured conical copper wire (SCCW) with controllable conicity, where the electrochemical etching time was accurately controlled by programmably moving the working electrode. It is demonstrated that liquid droplets could move in a self-propelled way along the SCCW and be balanced at certain position, making SCCW an excellent fibrous medium to manipulate liquid. Of note, the SCCW with the apex angle of 4.2° is capable of manipulating/transferring liquid whose volume is up to 428 times its own volume when it was placed with a tilt angle of 24°, which is even higher than that of FE-hairs (~180 times). Thus, we believe that the bio-inspired SCCWs and their ability in highly efficient liquid handling reported in this contribution may shed some light on the development of novel fibrous devices for controllable and highly efficient liquid manipulation.

RESULTS AND DISCUSSION

SCCWs with different topographies were fabricated in one step by a dynamic electrochemical method, as schematically shown in Figure 1d,e. Briefly, as shown in Figure 1d, a cylindrical copper wires with diameter of approximately 250 μm were fixed on a programmable moving apparatus at one end, and the other end was immersed into $CuSO_4$ (0.15 M) electrolyte solution which operated as the working electrode (anode) for electrochemical corrosion. Another polished copper sheet (1 cm × 5 cm) was coaxially surrounding the copper wire, working as the counter electrode (cathode). When the working electrode was moved at a certain speed, the structured copper wire with conical shape could be successfully prepared (Figure 1f). Importantly, we found that the surface morphology of the SCCW could be accurately controlled by reciprocating the working electrode at different speeds. For a large velocity (v > 0.1 mm/s in our experiment), the speed of the moving copper wire is much bigger than that of corrosion rate, minimizing the occurrence of corrosion on the surface of the cylindrical wires in each corrosion cycle, and as a consequence, the SCCW with smooth surface morphology was obtained (Figures S1a and S2a). In contrast, for a small velocity (v < 0.02 mm/s in our experiment), the contact time of the electrode and electrolyte increased, resulting in intensive corrosion on the surface of the wires, and therefore, the SCCW with a rough surface composed of many structured scales was successfully fabricated (Figures S1b and S2b).

The scanning electron microscopy (SEM) images of a SCCW illustrate its hierarchical micro-/nanostructures, as presented in Figure 1f−h. We found that the SCCW shows a conical structure with gradual changes in radius from ~100 nm for its tip to ~250 μm for the base along the wire axis (Figure 1f). Magnified images (Figure 1g) reveal a large quantity of micrometer scaled grooves on the surface of the SCCW. Worth noting is that these grooves are composed of numerous nanostructured scales (Figure 1h), exhibiting similar dimensions as those of the oriented squamae of FE-hairs in Chinese brushes.[28] We considered that the hierarchical micro-/nanostructures of the SCCW, featured by the conical architecture with micrometer scaled grooves and nanostructured scales, could give rise to a surface energy gradient and a difference in Laplace pressure,[28] which may contribute to the highly efficient liquid manipulation ability of the SCCW.

Moreover, by controlling the length of the wire immersed into the electrolyte (initial etchant length, L_i), we successfully fabricated SCCWs with various apex angles, 2α, in a well-controllable way (Figure 1i). Specifically, the SCCW with apex angle of ~4.2° can be obtained if the L_i of cylindrical copper wire was 5 mm, while the SCCW with apex angles of ~14.7° can be successfully fabricated if L_i is equal to 1 mm. In traditional chemical etching technique,[34] the electrolyte is static, and therefore, the short taper structure was usually formed because the height of the liquid meniscus was reduced with the decrease of the wire diameter during etching (Figure S3). The traditional chemical etching technique suffers from the poor reproducibility and controllability for making conical tips with certain structures. To overcome these limitations, herein, we propose the use of a programmable moving electrode with a control apparatus to realize the precise control of the conical structure and the surface morphology of the SCCWs (Figure 1), as well as the ability to handle liquid droplets in various ways.

When silicon oil (surface tension, γ = 20 mN/m) drops were released at the surface of the SCCW, they could exhibit self-propelled movement behavior along the SCCW (Figures S4−S7) driven by the Laplace pressure difference, ΔP, arising from conical structures,[29] and finally stopped at certain position where the ΔP was balanced by the retention force and the gravity (or the component of the gravity in case the SCCW is not perpendicularly placed). Like Chinese brushes, the droplets with same volume (V) would always stop and be balanced at the same position (balance position) no matter where they were released (Figure 2a). If a drop of silicon oil was placed at the tip of the SCCW, it would spontaneously move upward from the tip to the region of lower curvature at a decreasing velocity as drop moving (black dotted line in Figure 2a and the bottom inset screenshots) because the ΔP generated in this region is much bigger than the gravity. In contrast, when a silicon oil droplet was released at the top of the SCCW where the local radius variation is much smaller, the as-generated ΔP is too small to propel the droplet to move upward. As a result, the droplet would move downward to the region of higher curvature (red dotted line in Figure 2a and the

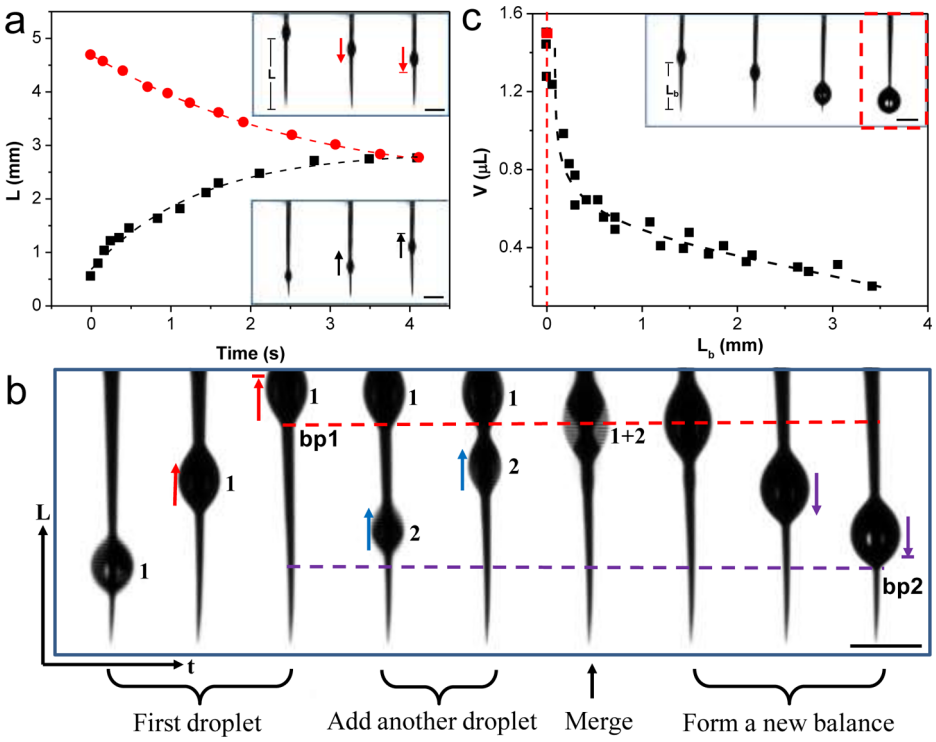

Figure 2. Dynamic balance of drops on the surface of SCCW. (a) When drops with same volume were placed on the surface of SCCW, they could exhibit self-propelled movement behavior and be balanced at the same position no matter at the tip (black dotted line) or the top (red dotted line) of SCCW. (b) Dynamic manipulation of drops on SCCW: when a silicon oil drop (drop 1) was released at the tip of SCCW, it would spontaneously move upward to the region of lower curvature and be balanced at one "balance position" (bp1, red dotted line). Then, when another drop was added (drop 2) to the tip area of SCCW, it would also move upward from the tip to the region of lower curvature, and then coalesce with the pre-existing drop 1 to form a new big drop (drop 1 + 2). After coalescence, this new drop moved downward and was finally balanced at a new "balance position" (bp2, purple dotted line). (c) For a fixed vertical SCCW, the balance position shows inversely proportional to the liquid volume. Scale bar is 1 mm.

top inset screenshots). Finally, silicon oil droplets with constant volume would stop at the same position whether it was released at the tip or the top of the SCCW. It demonstrated that the SCCW enables holding/manipulating a liquid droplet steadily.

More importantly, we found that the balance behavior of the liquid on the surface of the SCCW is a dynamic process (Figure 2b), and the efficiency in liquid holding for a single SCCM is varied at the different balanced positions (Figure 2c). Here, we suggested that making the balanced position at the tip area (*i.e.*, L_b approaching 0, namely, the boundary condition) enables highest efficiency in liquid holding for a single SCCW. When a silicon oil droplet was placed (drop 1) at the tip of SCCW, it would move upward and finally be balanced at a "balance position 1" (bp1, red dotted line in Figure 2b). Then, when another drop (drop 2) was added to the same region of the SCCW, it would also move upward from the tip to the base of the SCCW. When it met with the pre-existing drop 1, two droplets would coalescence to form a new big drop (drop 1 + 2). After they merged, this new big drop moved downward since its gravity increased. Finally, it stopped and was balanced at a new "balance position 2" (bp2, purple dotted line in Figure 2b), a position much closer to the tip of the SCCW. The liquid manipulation process indicated that the balance position of drop on the surface of the SCCW showed significant dependence on the drop volume. It could be further evidenced by monitoring the dynamic balance behavior of the drop on the surface of SCCW by measuring the distance of the balance position away from the tip, L_b, *versus* drop volumes, *V*, as plotted in Figure 2c. We found that for small *V* (*ca.* $V < 0.7\ \mu$L), the L_b shows a quick decrease with the enlargement of the drop volume, whereas it presented a slow decrease with increased liquid volume for a large volume region (*ca.* $V > 0.7\ \mu$L), where the drops were balance around the tip region of the SCCW. It is clearly suggested that the L_b shows inversely proportional to the liquid volume held by a single SCCM for a certain SCCW, and the boundary condition of L_b approaching 0 enables highest efficiency in liquid holding.

As a boundary condition to balance the liquid droplet dynamically, the tip region of the SCCW could hold much amount of liquid, compared with that of other positions along the SCCW (Figure 2c). Thus, we assume that the maximum volume (V_{max}) of drop that can be held on the tip of the SCCW is the maximum liquid capacity of SCCW. We found that changing the

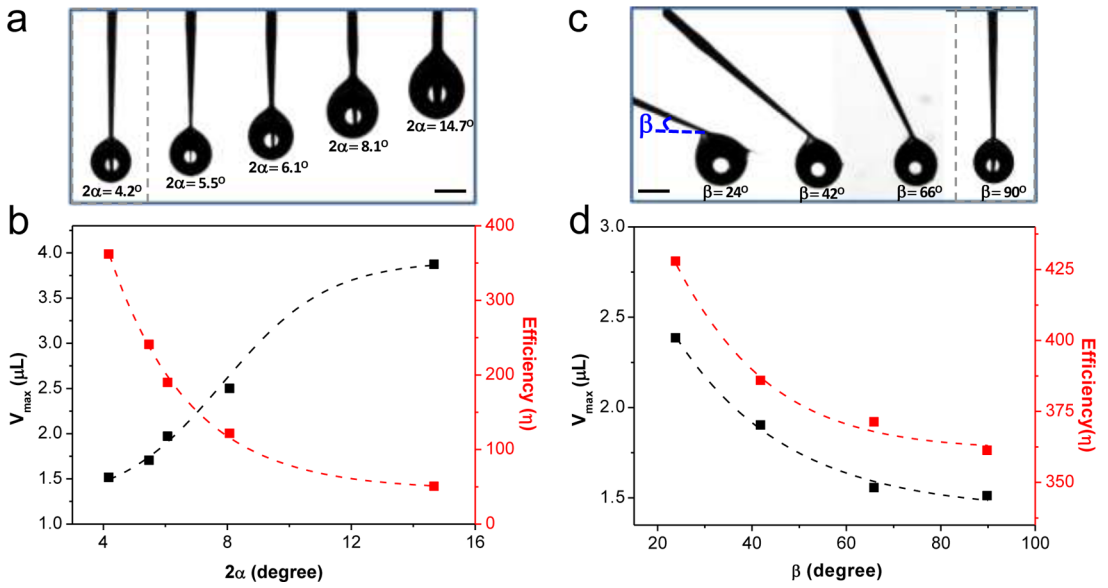

Figure 3. Highly efficient liquid transfer of SCCW. (a and b) For vertical SCCWs with different apex angles (2α), the maximum volume (V_{max}, black dotted line) of drop that can be held on the tip of SCCW is reversed to apex angle (2α), while the efficiency of liquid transfer (η, red dotted line) shows positive correlation with apex angle (2α). (c and d) For SCCWs with certain apex angle (2α = 4.2°) but different tilt angles (β), both the maximum volume of holding drop (V_{max}, black dotted line) and the efficiency of liquid transfer (η, red dotted line) decrease with the increase of tilt angle (β). Scale bar is 1 mm.

apex angles of SCCW, 2α, can significantly alter the maximum liquid capacity of SCCW, as summarized in Figure 3a. The SCCW with apex angle of 4.2° can hold a droplet of 1.5 μL. The maximum liquid capacity of SCCW with apex angles of 5.5°, 6.1°, 8.1°, and 14.7° is 1.7, 2.0, 2.5, and 3.9 μL, respectively, which suggested that the liquid holding ability increases with the enlargement of the apex angle of SCCW (black line in Figure 3b). Moreover, we also found that the tilt angle, β, can affect the maximum liquid capacity of SCCW. As presented in Figure 3c,d, the maximum liquid capacity of SCCW showed inversely proportional to the tilt angle (black line in Figure 3d). Specifically, for an apex angle of 4.2°, the SCCW with a tilt angle of 24° can store 2.4 μL of silicon oil droplet, about 60% weight enhancement comparing with the liquid droplet of 1.5 μL that was held by a vertically placed SCCW (β ~ 90°). Here, we revealed the direct relationship of topography of the conical fiber and its ability in handling liquid quantitatively, and more importantly, we suggested that the way of conical fiber interacting with liquid droplet (*i.e.*, the title angle), can also significantly alter its ability in manipulating liquid.

To better understand the ability to manipulate liquid for the SCCW, we use η ($\eta = V_1/V_2$) to evaluate the efficiency of liquid manipulated by a SCCW, where V_1 is the volume of liquid droplet and V_2 is the volume of SCCW that was encapsulated by the liquid. It is found that the SCCW exhibits an amazing ability of manipulating liquid droplet with a rather high volume, and a SCCW with apex angles of 4.2° can store more than 350 times its own volume of liquid (η = 361), as shown in Figure 3b (red line). In contrast, for the SCCW with an apex angle of 14.7°, the efficiency of liquid transfer is ~50. Although the absolute value of the maximum liquid capacity for a SCCW decreased when the apex angle was reduced, the efficiency of liquid transfer presented prominent increase as the apex angle decreased. For a drop at the tip of the vertically placed SCCW, the droplet is approximately spherical. Thus, the droplet volume can be express as $V_1 \sim [(4/3)\pi R^3]$, while the encapsulated SCCW volume is $V_2 \sim [(1/3)\pi r^2 \times 2R] \sim [(8/3)\pi R^3\alpha^2]$. Therefore, the efficiency follows the relationship of $\eta \sim 0.5\alpha^{-2}$, which show inversely proportional to apex angle of the SCCW (Figure S8). Meanwhile, the efficiency of liquid manipulation was also affected by the placement of the SCCW. Decreasing the tilt angle could significantly enhance the efficiency of liquid manipulation, as presented in Figure 3d (red line). We noted that up to 400 times of its own volume of liquid (η = 428) can be held by the SCCW (2α = 4.2°) with a tilt angle of 24° (Figure 3d). These results clearly demonstrated that a decrease in the tilt angle or increase in the apex angle enables the SCCW to manipulate liquid with high efficiency.

For a drop held at the tip region of a SCCW, there are three main forces working on it (Figure 4a): a holding force arising from Laplace pressure difference F_l,[29] the component of the gravity F_g, which can be expressed as $\rho gV \sin\beta$; and the retention force arising from surface microstructures F_r, which can be approximated as $k\rho gV \sin\beta$, where k is an arbitrary constant associated with the surface structure of SCCW.[35] The net force can be approximately expressed as $F \sim F_l + F_r - \rho gV \sin\beta$. When a drop was balanced at the tip of SCCW, the holding force F_l is the gradient of ΔP

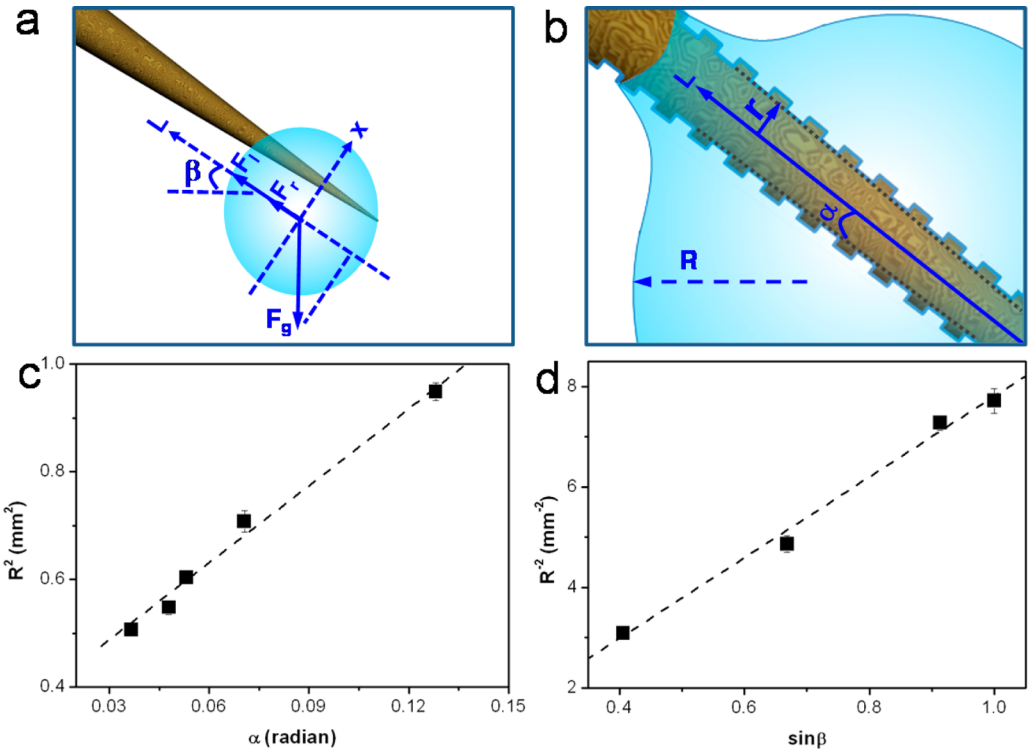

Figure 4. Mechanism of maximum liquid capacity of SCCW. (a) For a drop held at the tip of SCCW with certain tilt angle (β), there are three main forces working on it: a holding force arising from Laplace pressure difference (F_l), component of the gravity F_g, and retention force (F_r) arising from surface structures of SCCW. (b) SCCW could generate two holding forces: Laplace pressure difference force (F_l) induced by the conical feature of SCCW and retention force (F_r) arising from rough structure. For SCCW with different apex angles (2α), the F_l can be obtained by integrating the Laplace pressure difference times the area around the entire liquid surface, and can be express as $F_l \sim [2\gamma \tan \alpha/(r + R)^2]V$. (c and d) The experimental (solid square) and theoretical (dotted line) results on the effect of 2α and β of SCCW on the liquid holding ability at the tip of SCCW. Here, α shows directly proportional to R^2, while sin β presents a linear relationship with R^{-2}.

induced by the conical feature of SCCW,[29] which can be obtained by integrating ΔP times the area around the entire liquid surface, $F_l \sim [2\gamma \tan \alpha/(r + R)^2)]V$ (Figure 4a,b). For a droplet on the tip region of the SCCW, the Laplace pressure that acts on it is much larger than that which acts on the top region, because the local curvature variation at the tip region is much bigger than that at the top region.[12,24,25] Thus, the ΔP can generate a large force to hold a big drop at the tip of the SCCW. Another possible driving force favorable for the liquid holding on a single SCCW is assignable to the unique micro-/nanosurface structures of the SCCW, which could generate a retention force to hold the liquid (Figure 4a) and was beneficial for the pining of three-phase contact line when interacting with liquid as illustrated in Figure 4b.

To comprehensive understand the mechanism of the maximum liquid capacity of the SCCW, we also considered the effect of tilt angle and apex angle of the SCCW on the liquid holding ability at the tip region of the SCCW. For vertical SCCWs (where $\beta = 90°$) with different apex angles, the force generated from ΔP could be balanced by the retention force and the gravity, thus giving a relationship of $[2\gamma \tan \alpha)/(r + R)^2]V \sim (1 - k)\rho gV$. When $R \gg r$ and $\alpha \ll 1$, we can get $\alpha \sim R^2$. We performed a series of experiments to examine the effect of the α on the R^2, and results show that R^2 is linearly proportional to α, presenting a good agreement with our theoretical calculation (Figure 4c). Similarly, for a SCCW with different β, the Laplace pressure difference force could be balanced by the retention force and the component of gravity, and thus, the net force can be express as $[2\gamma \tan \alpha)/(r + R)^2]V \sim (1 - k)\rho gV \sin \beta$. When $R \gg r$, we can get $\sin \beta \sim R^{-2}$. Experimental data present an excellent support to our theoretical results as given in Figure 4d.

CONCLUSIONS

In conclusion, inspired by the controllable liquid transfer of the Chinese brushes, we developed a facile dynamic electrochemical corrosion method to fabricate the SCCWs with controllable conicity and surface morphology. The as-prepared SCCWs exhibited a typical hierarchical multistructured topology upon programmably controlling the motion of the electrode. The SCCWs exhibit unique abilities in handling liquid because of their unique dynamic liquid balance behavior, resembling that of FE-hairs. Worth noting is that the highly efficient liquid manipulation ability was realized by using the boundary condition of the dynamic liquid balance behavior at the tip region of the SCCW. When cooperatively controlling the tilt angle

and apex angle of the SCCW, we can manipulate a large mass of liquid in a well-controllable manner. We first identified that a decrease in the tilt angle or increase in the apex angle enables the SCCW to manipulate liquid with a rather high efficiency, which is over 428 times greater than its own volume. We therefore anticipate that this bio-inspired SCCW could provide new insight in designing novel materials and devices to manipulate liquid in a more controllable way and with high efficiency.

EXPERIMENTAL SECTION

Preparation of Structured Conical Copper Wires (SCCWs). Copper wires with conical architecture enveloped by structured scales were prepared by a dynamic electrochemical method. First, commercial copper wires with diameter of approximately 250 μm were washed successively with a 1.0 M HCl aqueous solution, acetone, and ethanol for 10 min each under ultrasonication. Subsequently, the copper wires were connected to the anode of a 10 V DC power supply and fixed on a programmed move apparatus, and the other end was immersed in an electrolytic cell setting as the working electrode (anode) for electrochemical corrosion. Another polished copper sheet (1 cm $\times$ 5 cm) was coaxially surrounding the copper wire and immersed in the electrolyte solution, setting as the counter electrode (cathode). The electrolyte was an aqueous solution containing $CuSO_4$ (0.15 M). When the electrolyte was moved up and down at a specific speed, the copper wires with structured conical shape could be successfully prepared.

Characterization of the Microstructures of the SCCW. The optical images of the SCCWs were recorded by a digital video camera (WV-CP280/CH, Panasonic, Japan). The microstructures of the SCCWs were observed by a field-emission scanning electron microscope (JEOL, JSM-6700F, Japan).

Experiments on the Liquid Manipulation. In our experimental study, the as-prepared SCCWs were arranged with the top end clamped and the bottom end free. Silicon oil drops (surface tension, γ = 20 mN/m) of known volume (ranging from 0.2 to 4 μL) were injected *via* precision tips (Nordson Corporation) onto the different regions of the SCCWs. A high-speed video camera (HCC-1000F) recorded the whole drop dynamics process.

Conflict of Interest: The authors declare no competing financial interest.

Supporting Information Available: Optical images of conical copper wires with smooth (a) and rough (b) morphology by using dynamic electrochemical method; SEM images of conical copper wires with smooth (a) and rough (b) surface; SEM image of the copper wire with short taper structure that fabricated by traditional static chemical etching technique; self-propelled movement behavior of silicon oil droplet on the surface of SCCW; the effect of apex angle (2α) of SCCW on the self-propulsion of droplets on the surface of SCCW; the effect of tilt angles (β) of SCCW on the self-propulsion of droplets on the surface of SCCW; the influence of drop volume (V) on the motion behavior of drop on vertical SCCW; experimental (black solid square) and theoretical (red line, $\eta = 0.5\alpha^{-2}$) relationship between $0.5\alpha^{-2}$ and η. This material is available free of charge *via* the Internet at http://pubs.acs.org.

Acknowledgment. The authors thank the financial support by National Research Fund for Fundamental Key Projects (2013CB933000), Program for New Century Excellent Talents in University (NCET-13-0024), Fok Ying Tong Education Foundation (132008), National Natural Science Foundation (61227902, 21121001, 91127025), the Key Research Program of the Chinese Academy of Sciences (KJZD-EW-M01), the 111 Project (No. B14009), and the Fundamental Research Funds for the Central Universities (YWF-14-HXXY-015).

REFERENCES AND NOTES

1. Ferraro, P.; Coppola, S.; Grilli, S.; Paturzo, M.; Vespini, V. Dispensing Nano-Pico Droplets and Liquid Patterning by Pyroelectrodynamic Shooting. *Nat. Nanotechnol.* **2010**, *5*, 429–435.
2. Ledesma-Aguilar, R.; Nistal, R.; Hernández-Machado, A.; Pagonabarraga, I. Controlled Drop Emission by Wetting Properties in Driven Liquid Filaments. *Nat. Mater.* **2011**, *10*, 367–371.
3. Park, J.-U.; Hardy, M.; Kang, S. J.; Barton, K.; Adair, K.; kishore Mukhopadhyay, D.; Lee, C. Y.; Strano, M. S.; Alleyne, A. G.; Georgiadis, J. G. High-Resolution Electrohydrodynamic Jet Printing. *Nat. Mater.* **2007**, *6*, 782–789.
4. Tian, D.; Chen, Q.; Nie, F. Q.; Xu, J.; Song, Y.; Jiang, L. Patterned Wettability Transition by Photoelectric Cooperative and Anisotropic Wetting for Liquid Reprography. *Adv. Mater.* **2009**, *21*, 3744–3749.
5. Fenn, J. B. Electrospray Wings for Molecular Elephants (Nobel Lecture). *Angew. Chem., Int. Ed.* **2003**, *42*, 3871–3894.
6. Tavana, H.; Jovic, A.; Mosadegh, B.; Lee, Q.; Liu, X.; Luker, K.; Luker, G.; Weiss, S.; Takayama, S. Nanolitre Liquid Patterning in Aqueous Environments for Spatially Defined Reagent Delivery to Mammalian Cells. *Nat. Mater.* **2009**, *8*, 736–741.
7. Wang, J.; Gao, W. Nano/Microscale Motors: Biomedical Opportunities and Challenges. *ACS Nano* **2012**, *6*, 5745–5751.
8. Su, B.; Wu, Y.; Jiang, L. The Art of Aligning One-Dimensional (1D) Nanostructures. *Chem. Soc. Rev.* **2012**, *41*, 7832–7856.
9. Su, B.; Wang, S.; Ma, J.; Wu, Y.; Chen, X.; Song, Y.; Jiang, L. Elaborate Positioning of Nanowire Arrays Contributed by Highly Adhesive Superhydrophobic Pillar-Structured Substrates. *Adv. Mater.* **2012**, *24*, 559–564.
10. Wu, Y.; Chen, X.; Su, B.; Song, Y.; Jiang, L. Elaborately Aligning Bead-Shaped Nanowire Arrays Generated by a Superhydrophobic Micropillar Guiding Strategy. *Adv. Funct. Mater.* **2012**, *22*, 4569–4576.
11. Duprat, C.; Protiere, S.; Beebe, A.; Stone, H. Wetting of Flexible Fibre Arrays. *Nature* **2012**, *482*, 510–513.
12. Li, K.; Ju, J.; Xue, Z.; Ma, J.; Feng, L.; Gao, S.; Jiang, L. Structured Cone Arrays for Continuous and Effective Collection of Micron-Sized Oil Droplets from Water. *Nat. Commun.* **2013**, *4*, 2276.
13. Tang, Y.; Yeo, K. L.; Chen, Y.; Yap, L. W.; Xiong, W.; Cheng, W. Ultralow-Density Copper Nanowire Aerogel Monoliths with Tunable Mechanical and Electrical Properties. *J. Mater. Chem. A* **2013**, *1*, 6723–6726.
14. Anzenbacher, P.; Palacios, M. A. Polymer Nanofibre Junctions of Attolitre Volume Serve as Zeptomole-Scale Chemical Reactors. *Nat. Chem.* **2009**, *1*, 80–86.
15. Millman, J. R.; Bhatt, K. H.; Prevo, B. G.; Velev, O. D. Anisotropic Particle Synthesis in Dielectrophoretically Controlled Microdroplet Reactors. *Nat. Mater.* **2005**, *4*, 98–102.
16. Song, H.; Chen, D. L.; Ismagilov, R. F. Reactions in Droplets in Microfluidic Channels. *Angew. Chem., Int. Ed.* **2006**, *45*, 7336–7356.
17. Teh, S.-Y.; Lin, R.; Hung, L.-H.; Lee, A. P. Droplet Microfluidics. *Lab Chip* **2008**, *8*, 198–220.
18. Dong, Z.; Ma, J.; Jiang, L. Manipulating and Dispensing Micro/Nanoliter Droplets by Superhydrophobic Needle Nozzles. *ACS Nano* **2013**, *7*, 10371–10379.
19. Rossi, M. P.; Ye, H.; Gogotsi, Y.; Babu, S.; Ndungu, P.; Bradley, J.-C. Environmental Scanning Electron Microscopy Study of Water in Carbon Nanopipes. *Nano Lett.* **2004**, *4*, 989–993.

20. Bai, H.; Ju, J.; Zheng, Y.; Jiang, L. Functional Fibers with Unique Wettability Inspired by Spider Silks. *Adv. Mater.* **2012**, *24*, 2786–2791.
21. Kang, E.; Jeong, G. S.; Choi, Y. Y.; Lee, K. H.; Khademhosseini, A.; Lee, S.-H. Digitally Tunable Physicochemical Coding of Material Composition and Topography in Continuous Microfibres. *Nat. Mater.* **2011**, *10*, 877–883.
22. Tang, Y.; Gong, S.; Chen, Y.; Yap, L. W.; Cheng, W. Manufacturable Conducting Rubber Ambers and Stretchable Conductors from Copper Nanowire Aerogel Monoliths. *ACS Nano* **2014**, *8*, 5707–5714.
23. Huang, J. Y.; Lo, Y.-C.; Niu, J. J.; Kushima, A.; Qian, X.; Zhong, L.; Mao, S. X.; Li, J. Nanowire Liquid Pumps. *Nat. Nanotechnol.* **2013**, *8*, 277–281.
24. Zheng, Y.; Bai, H.; Huang, Z.; Tian, X.; Nie, F.-Q.; Zhao, Y.; Zhai, J.; Jiang, L. Directional Water Collection on Wetted Spider Silk. *Nature* **2010**, *463*, 640–643.
25. Ju, J.; Bai, H.; Zheng, Y.; Zhao, T.; Fang, R.; Jiang, L. A Multi-Structural and Multi-Functional Integrated Fog Collection System in Cactus. *Nat. Commun.* **2012**, *3*, 1247.
26. Bai, H.; Tian, X.; Zheng, Y.; Ju, J.; Zhao, Y.; Jiang, L. Direction Controlled Driving of Tiny Water Drops on Bioinspired Artificial Spider Silks. *Adv. Mater.* **2010**, *22*, 5521–5525.
27. Ju, J.; Xiao, K.; Yao, X.; Bai, H.; Jiang, L. Bioinspired Conical Copper Wire with Gradient Wettability for Continuous and Efficient Fog Collection. *Adv. Mater.* **2013**, *25*, 5937–5942.
28. Wang, Q.; Su, B.; Liu, H.; Jiang, L. Chinese Brush: Controllable Liquid Transfer in Ratchet Conical Hairs. *Adv. Mater.* **2014**, *26*, 4889–4894.
29. Lorenceau, E.; Quere, D. Drops on a Conical Wire. *J. Fluid Mech.* **2004**, *510*, 840PJ.
30. Bhushan, B. Nanoscale Characterization of Human Hair and Hair Conditioners. *Prog. Mater. Sci.* **2008**, *53*, 585–710.
31. Extrand, C. Retention Forces of a Liquid Slug in a Rough Capillary Tube with Symmetric or Asymmetric Features. *Langmuir* **2007**, *23*, 1867–1871.
32. Zheng, Y.; Gao, X.; Jiang, L. Directional Adhesion of Superhydrophobic Butterfly Wings. *Soft Matter* **2007**, *3*, 178–182.
33. Liu, C.; Ju, J.; Zheng, Y.; Jiang, L. Asymmetric Ratchet Effect for Directional Transport of Fog Drops on Static and Dynamic Butterfly Wings. *ACS Nano* **2014**, *8*, 1321–1329.
34. Kulakov, M.; Luzinov, I.; Kornev, K. Capillary and Surface Effects in the Formation of Nanosharp Tungsten Tips by Electropolishing. *Langmuir* **2009**, *25*, 4462–4468.
35. Malvadkar, N. A.; Hancock, M. J.; Sekeroglu, K.; Dressick, W. J.; Demirel, M. C. An Engineered Anisotropic Nanofilm with Unidirectional Wetting Properties. *Nat. Mater.* **2010**, *9*, 1023–1028.